Natural Hazards **27:** 105–131, 2002.

Site-Specific Analysis of Strong Motion Data from the September 7, 1999 Athens, Greece Earthquake

G. D. BOUCKOVALAS and G. P. KOURETZIS
National Technical University of Athens, Greece

I. S. KALOGERAS
National Observatory of Athens, Institute of Geodynamics

Received: 22 August 2000; accepted in revised form: 30 March 2001

Abstract. The strong ground motion from Athens, Greece 07/09/1999 earthquake has been recorded by eighteen (18) stations, fourteen (14) within the central Athens area and four (4) at the centers of nearby towns. The ground conditions for most of the recording sites were identified, based on previous geotechnical investigations carried out in the wider area of the sites, and consequently correlated to the seismic motion characteristics. Hence, it has been possible to evaluate the accuracy of different seismological methods for site characterization and also estimate soil effects on peak ground acceleration and elastic response spectra. In addition, preliminary estimates are drawn for the seismic motion characteristics at the epicentral area, where no strong motion recordings are available. The detailed soil profiles at the recording sites are placed in the Appendix.

Key words: Earthquakes, seismic recordings, site characterization, soil effects

1. Introduction

Athens, Greece earthquake of 07/09/1999 occurred at 11:56:50.5 GMT at the western bounds of the greater metropolitan area of Athens. Hence, despite its moderate magnitude of 5.9 and the medium focal depth of 16.8 km (Papadopoulos *et al.*, 2000) it caused the loss of 143 lives, the collapse of about 100 buildings and the severe damage of another 13,000. In fact, this earthquake is the first ever reported to have caused casualties within the urban area of Athens and it can be certainly considered as the worst natural disaster in the modern history of Greece.

The strong ground motion from the mainshock of the earthquake has been recorded by eighteen (18) accelerographs, fourteen (14) within the central area of Athens and four (4) at the center of nearby towns of Rafina, Lavrio, Aliveri and Thiva. The bulk of the recordings was due to the accelerograph network operated by the Geodynamic Institute of the National Observatory of Athens (NOAGI) (Kalogeras and Stavrakakis, 1999), while a number of the recordings was obtained at accelerograph stations maintained by the Institute of Engineering Seismology and Earthquake Engineering (ITSAK) and the Public Power Corporation (DEI). It is fortunate that most of the recording sites lay in the vicinity of major public works,

such as surface or underground stations of the Athens subway system (METRO). Thus, it has been possible to collect data from previous geotechnical investigations and define the local ground conditions at the recording sites.

Essentially, this additional information allowed us to treat the seismological data as results from a natural scale experiment aimed at the investigation of local soil effects on peak seismic motion parameters and frequency content. In addition, it provided the means to estimate the seismic ground motion characteristics at the epicentral area where no main shock recordings are available. More specifically, the following important issues are addressed in this article: (a) the principal direction of ground shaking, (b) the accuracy of pure seismological methods for site characterization, (c) the effect of local soil conditions on peak ground accelerations and elastic response spectra, and (d) the seismic motion characteristics at the epicentral area which suffered the most severe damages and the heaviest casualties.

2. Documentation of Seismic Recordings

Figure 1 and Table I summarize basic information regarding the rupture mechanism of Athens, Greece earthquake and the recorded strong ground motions. Namely, Figure 1 shows the:

- epicenter of the main shock of September 7th 1999, announced by NOAGI,
- epicenters of aftershocks recorded during the period September 8th October 29th 1999, based on NOAGI local array recordings,
- traces of two active faults (Fili and Aspropyrgos faults), which bound the aftershock epicenters from the north and also exhibit similar geometry to the main rupture plane (Papadopoulos *et al.*, 2000), and
- location of the recording sites for the main shock.

Furthermore, Table I summarizes the:

- recorded peak ground accelerations and velocities,
- distance of recording sites from the fault rupture, assumed to lay between Fili and Aspropyrgos faults,
- direction of the maximum peak ground acceleration relative to the north, deduced from composition of the two horizontal components (LONG and TRANS) of recorded acceleration time histories,
- predominant periods of shaking deduced from the two horizontal components of recorded acceleration time histories,
- geological conditions prevailing at the recording sites, as well as,
- information regarding the location of the seismographs with regard to the ground surface and nearby massive structures.

All recordings sites, except from that in the town of Thiva (THVC in the map of Figure 1), lay to the east of the rupture zone and on the hanging wall side of the fault. Furthermore, they correspond to a wide range of fault distances, between 9 and 52 km, and consequently they may provide evidence for the attenuation of seismic motion with distance from the fault rupture. On the other hand, the local

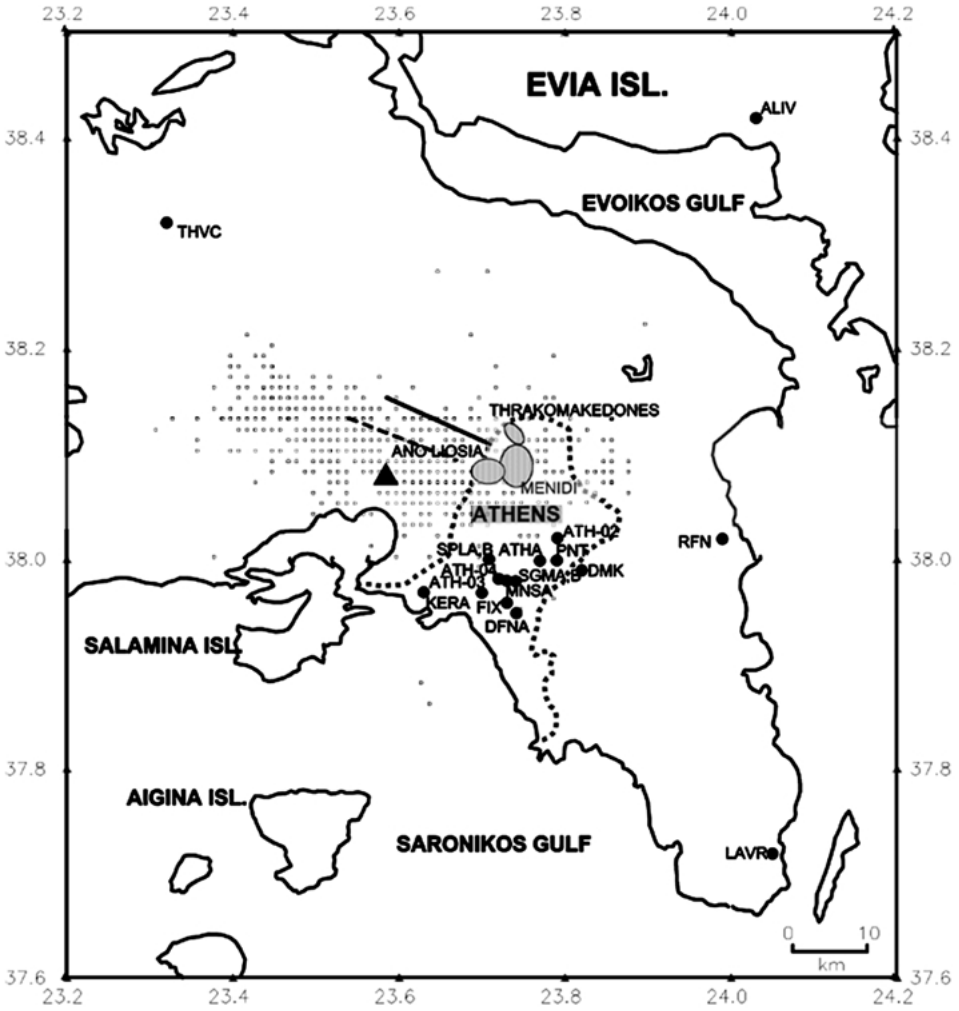

Figure 1. Map of the epicentral area of Athens 07/09/1999 earthquake. Hollow rectangles indicate aftershock epicenters for the period of 8 Sept. to 29 Oct. 1999, the triangle corresponds to the epicenter of the main shock, while black spots denote strong motion recording sites. The continuous and dashed lines represent the simplified traces of Fili and Aspropirgos faults respectively.

ground conditions are also variable, from limestone to dense alluvium, and may result in considerable scatter of the data unless soil effects are taken into account properly.

The direction of the maximum acceleration vector ranges between 45° and 180°N with an average (+ one standard deviation) direction of about 109° (+ 39°). This finding is also substantiated from observations at the cemeteries of the meizoseismal areas immediately after the earthquake, which revealed that marble

Table I. Documentation of strong seismic motion recordings.

Recording	Component	Distance from rupture (km)	a_{max} (g)	v_{max} (m/s)	Direction of a_{max}	Predominant period	Geological conditions	Location of instrument
ATHA (Neo Psihiko)	Long	12	0.084	0.053	60°N	0.18–0.27	Tertiary deposits	3-stories RC-private build.
	Trans		0.101	0.074		0.13–0.17		
	Vert		0.114	0.034		0.05–0.07		
MNSA (Monastiraki)	Long	13	0.229	0.149	110°N	0.12–0.22	Manmade deposits/schist/ phyllite	Free field-Metro station
	Trans		0.512	0.149		0.13–0.19		
	Vert		0.162	0.035		0.04–0.07		
SPLB (Sepolia)	Long	9	0.324	0.214	180°N	0.20–0.34	Manmade deposits/alluvium/ schist	3-story steel build.– Metro garage
	Trans		0.312	0.189		0.15–0.33		
	Vert		0.192	0.074		0.08–0.14		
DMK (Ag. Paraskevi)	Long	16	0.046	0.025	45°N	0.08–0.13	Limestone	Small RC house– Democritus Institute
	Trans		0.076	0.025		0.09–0.13		
	Vert		0.038	0.030		0.10–0.14		
ATH-02 (Chalandri)	Long	12	0.110	0.051	135°N	0.11–0.20	Alluvium/schist	2-stories RC build.– town hall
	Trans		0.159	0.069		0.08–0.25		
	Vert		0.092	0.034		0.08–0.11		
ATH-03 (Kallithea)	Long	13	0.264	0.161	100°N	0.09–0.13	Alluvium/schist	1-storey RC build.– K.E.D.E.
	Trans		0.303	0.147		0.19–0.26		
	Vert		0.157	0.070		0.04–0.07		
ATH-04 (Kipseli)	Long	12	0.121	0.089	90°N	0.09–0.11	Schist	3-stories RC build.– G.Y.S.
	Trans		0.110	0.085		0.11–0.30		
	Vert		0.053	0.034		0.07–0.12		
KERA (Keratsini)	Long	14	0.223	0.100	125°N	0.17–0.40	Tertiaty deposits	P.P.C. Power Plant
	Trans		0.186	0.073		0.20–0.27		
	Vert		0.155	0.042		0.06–0.13		
SPLA (Sepolia)	Long	9	0.255	0.179	135°N	0.09–0.13	Alluvium/schist	−2 level (−13 m)- Metro station
	Trans		0.221	0.128		0.19–0.52		
	Vert		0.082	0.059		0.05–0.07		
SGMA (Syntagma)	Long	13	0.149	0.127	100°N	0.10–0.18	Schist	−1 level (−7 m)- Metro station
	Trans		0.239	0.134		0.13–0.17		
	Vert		0.054	0.030		0.11–0.21		

Table I. Continued.

Recording	Component	Distance from rupture (km)	a_{max} (g)	v_{max} (m/s)	Direction of a_{max}	Predominant period	Geological conditions	Location of instrument
SGMB	Long	13	0.111	0.099	100° N	0.19–0.29	Schist	−3 level (−26 m)–
(Syntagma)	Trans		0.087	0.108		0.23–0.59		Metro station
	Vert		0.089	0.036		0.13–0.16		
DFNA (Dafni)	Long	16	0.045	0.044	55° N	0.12–0.23	Alluvium/schist	−2 level (−14 m)–
	Trans		0.080	0.077		0.16–0.25		Metro station
	Vert		0.041	0.028		0.11–0.18		
PNT (Papagou)	Long	13	0.088	0.076	140° N	0.16–0.25	Tertiary deposits	−2 level (−15 m)–
	Trans		0.079	0.051		0.15–0.27		Metro station
	Vert		0.055	0.038		0.08–0.11		
FIX	Long	15	0.086	0.079	70° N	0.17–0.22	Alluvium/schist	−2 level (−15 m)–
(Sygrou-Fix)	Trans		0.124	0.110		0.16–0.29		Metro station
	Vert		0.046	0.035		0.08–0.14		
RFN (Rafina)	Long	27	0.081	0.035	160° N	0.09–0.12	Tertiary deposits/	Small wooden house–
	Trans		0.100	0.053		0.09–0.15	limestone	private building
	Vert		0.030	0.029		0.04–0.11		
ALIV (Aliveri)	Long	47	0.020	0.009		0.20–0.23	Neogene marls	P.P.C. Power Plant
	Trans		0.017	0.009		0.11–0.23		
	Vert		0.010	0.005		0.10–0.14		
LAVR (Lavrio)	Long	52	0.042	0.020		0.06–0.11	Schist/limestone	P.P.C. Power Plant
	Trans		0.053	0.018		0.22–0.30		
	Vert		0.048	0.018		0.22–0.31		
THVC (Thiva)	Long	30	0.058	0.036	150° N	0.27–0.42	Conglomerate	3-story RC-town hall
	Trans		0.056	0.026		0.09–0.11		
	Vert		0.044	0.019		0.17–0.23		

decoration (crosses, etc) and tomb covers had slipped and overturned in a gross E-W direction.

Papadopoulos *et al.* (2000), based on P-wave polarities, were able to determine a fault plane solution indicating normal faulting and nodal planes with direction 113°N and 290°, dipping 56° to the northeast and 39° to the southwest, respectively. In light of these data, the predominant direction of the recorded ground motions appears more or less parallel to the nodal fault planes and perpendicular to the direction of the fault movement.

3. Site Characterization

A number of empirical methods are currently available to deduce directly the site characteristics from seismic recordings. This is an essential first step before proceeding with compilation of the strong motion data. In the present study, two of the most commonly applied methods are used for this purpose: the first based on the horizontal-to-vertical spectral ratio (HVSR) and the other based on the ratio of peak ground acceleration over peak ground velocity ($v_{\max}/a_{\max}$).

The HVSR method draws upon observations that soil conditions do not affect the vertical component of motion but only the horizontal, an assumption substantiated also by data of this study presented in later sections. Thus, dividing the spectra of the two horizontal components by the spectrum of the vertical component of the seismic ground motion you deduce a (type of) transfer function spectrum, reflecting the frequency characteristics of the soil column resting above the seismic bedrock. This method has been initially applied for quick, in situ estimates of the fundamental site period from the Fourier spectra of microtremors (Nakamura, 1989). Later, its use has been also extended to strong seismic motion recordings, with encouraging results (e.g., Theodoulidis *et al.*, 1996; Bonilla *et al.*, 1997; Yamazaki and Ansary, 1997; Dimitriou *et al.*, 1999; Trifunac and Todorovska, 2000a, b).

In the present study, the HVSR technique is applied to all strong motion recordings using the normalized elastic response spectra (for 5% damping) instead of the Fourier spectra mostly used in the literature. The reason for this modification, referred briefly here after as Normalized Horizontal-to-Vertical Spectral Ratio or NHVSR, is demonstrated in Figures 2 and 3, comparing NHVSR to HVSR for two typical recordings: THVC on neogene, soft rock formations and SPLB on dense alluvial deposits. Observe that the two spectral ratios are grossly similar, but HVSR is very sensitive to the amount of smoothing applied and cannot be interpreted as clearly as the NHVSR. Focusing on the NHVSR, it is further observed that not only its fundamental site period but also the peak of the spectral ratio increases, as the soil column becomes more flexible. Namely, the peak value increases from 2.13 to 4.85 as the fundamental period increases from 0.10 to 0.30 s. Note that the use of elastic response spectra instead of Fourier spectra, for quantitative estimates of frequency related soil parameters from seismic motions, is presently gaining ground

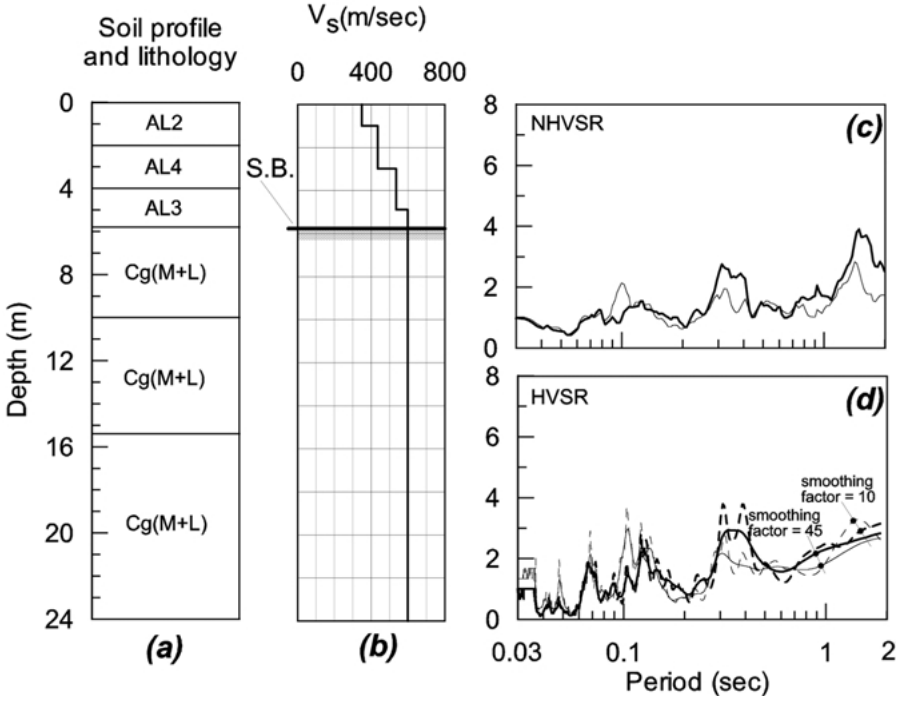

Figure 2. Classification of THVC recording site based on Horizontal to Vertical Spectral Ratios: (a) and (b) site profiles, (c) ratio of normalized response spectra, (d) ratio of Fourier Spectra. The bold lines correspond to the LONG and the thin lines to the TRANS component of motion. The notation of lithology is explained in the Appendix.

among engineers as well as seismologists (e.g., Joyner *et al.*, 1994; Mucciarelli *et al.*, 1996; Dobry *et al.*, 2000).

The second technique for site characterization, based on the $v_{\max}/a_{\max}$ ratio, draws upon the relation between $v_{\max}$ and $a_{\max}$ for harmonic motions:

$$v_{\max} = \frac{1}{\omega} \cdot a_{\max} \tag{1}$$

or

$$v_{\max}/a_{\max} = \frac{1}{2 \cdot \pi} T. \tag{2}$$

Thus, theoretically at least, the ratio of $v_{\max}/a_{\max}$ is proportional to the fundamental site period. Donovan (1989), working with empirical attenuation relations, has shown that this hypothesis is indirectly supported by seismological evidence. He further proposed to assign the average values of $v_{\max}/a_{\max}$ = 61 cm/s/g and 122 cm/s/g to "rock" and "soft soil" formations, respectively.

Table II summarizes the fundamental site period derived with the NHVSR method (T_{NHVSR}), the peak value of NHVSR (A_{NHVSR}) and the $v_{\max}/a_{\max}$ ratio

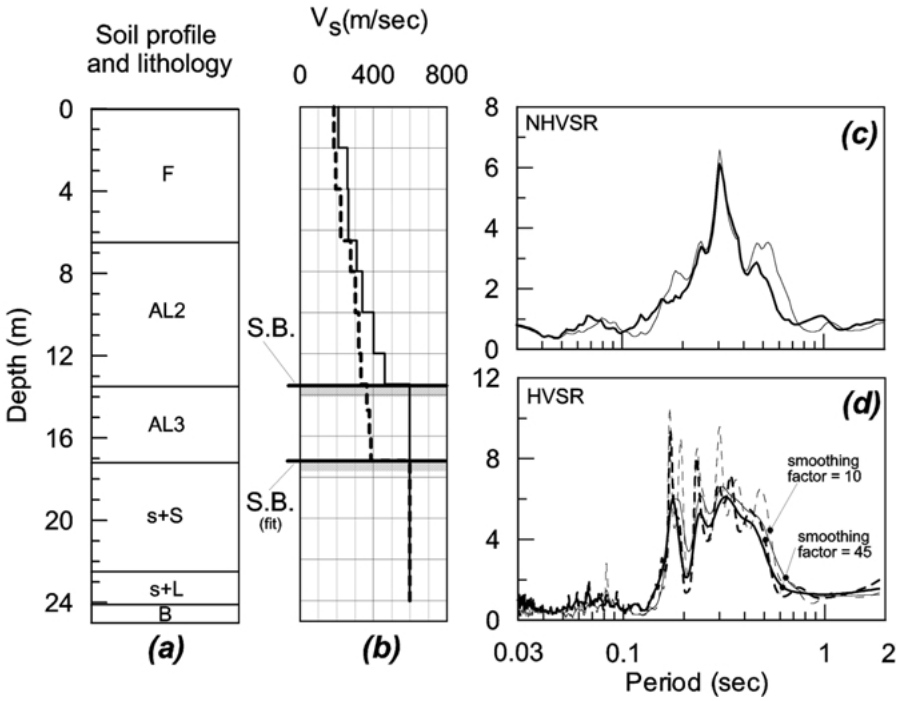

Figure 3. Classification of SPLB recording site based on Horizontal to Vertical Spectral Ratios. The presentation follows the format of Figure 2.

for the two horizontal components (LONG and TRANS) of the seismic ground motion at the recording sites. In addition, Figures 4a and 4b correlate the A_{NHVSR} and $v_{\max}/a_{\max}$ ratios to the fundamental site period T_{NHVSR} obtained from ground surface recordings. Both correlations are reasonably well established, exhibiting a coefficient of determination $r^2 = 0.91$ and $r^2 = 0.86$ for A_{NHVSR} and $v_{\max}/a_{\max}$ respectively. Furthermore, they show that among the three quantities, A_{NHVSR} is the most sensitive to soil conditions, while $v_{\max}/a_{\max}$ appears to be the least sensitive. More specifically, computing the range of variation for these variables as [standard deviation/average] ratio yields 0.63 for A_{NHVSR}, 0.45 for T_{NHVSR} and only 0.24 for $v_{\max}/a_{\max}$. It is noted that reported statistics for A_{NHVSR} were actually deduced from an analysis of $(A_{\mathrm{NHVSR}} - 1)$ values, taking into account that, by definition, $A_{\mathrm{NHVSR}} \approx 1$ at outcropping bedrock ($T_{\mathrm{NHVSR}} \approx 0.0$)

From a joint evaluation of these data and the local geological-geotechnical conditions, surface recording sites were classified in two categories:

(a) *Rock – Soft Rock formations*. It includes all sites with A_{NHVSR} less than 3, fundamental site periods T_{NHVSR} between 0.07 and 0.26 s, and $v_{\max}/a_{\max}$ ratio less than 58 cm s^{-1} g^{-1}. The geological formations belonging to this category are slightly to medium weathered phases of the Athens Schist (ATH-04 site), metamorphosed schist and limestone (DMK and LAVR sites), cohesive talus

Table II. Site characterization parameters obtained from the interpretation of seismic recordings

Recording	Component	Depth (m)	T_{NHVSR} (s)	v_{max}/a_{max} (cm s^{-1} g^{-1})	A_{NHVSR}	Soil category
ATHA	Long	0	0.32	63.72	3.74	SOIL
	Trans		0.31	73.79	3.48	SOIL
MNSA	Long	0	0.31	65.16	6.22	SOIL
	Trans		0.20	29.20	3.81	SOIL
SPLB	Long	0	0.30	65.98	4.46	SOIL
	Trans		0.30	60.63	4.85	SOIL
DMK	Long	0	0.11	53.87	1.33	ROCK
	Trans		0.15	32.61	1.47	ROCK
ATH-02	Long	0	0.30	46.31	3.77	SOIL
	Trans		0.14	43.53	2.36	ROCK
ATH-03	Long	0	0.24	61.08	2.80	ROCK
	Trans		0.22	48.51	3.16	SOIL
ATH-04	Long	0	0.48	73.55	2.71	ROCK
	Trans		0.48	77.59	2.31	ROCK
KERA	Long	0	0.31	44.67	3.25	SOIL
	Trans		0.32	39.14	3.32	SOIL
SPLA	Long	13	0.28	70.19	2.37	–[1]
	Trans		0.28	58.10	1.76	–[1]
SGMA	Long	7	0.12	85.25	1.82	–[1]
	Trans		0.16	55.86	1.68	–[1]
SGMB	Long	26	0.34	89.70	4.29	–[1]
	Trans		0.36	123.59	3.87	–[1]
DFNA	Long	13.5	0.21	98.92	2.15	–[1]
	Trans		0.22	95.92	1.82	–[1]
PNT	Long	15	0.29	85.70	1.99	–[1]
	Trans		0.29	64.36	2.82	–[1]
FIX	Long	15	0.23	91.68	1.97	–[1]
	Trans		0.23	88.55	1.98	–[1]
RFN	Long	0	0.12	43.87	2.15	ROCK
	Trans		0.14	53.03	1.67	ROCK
ALIV	Long	0	0.22	45.89	1.56	ROCK
	Trans		0.17	54.80	2.36	ROCK
LAVR	Long	0	0.09	46.78	2.50	ROCK
	Trans		0.08	33.84	2.31	ROCK
THVC	Long	0	0.31	61.60	2.75	ROCK
	Trans		0.10	46.75	2.13	ROCK

[1] Underground recordings are not classified.

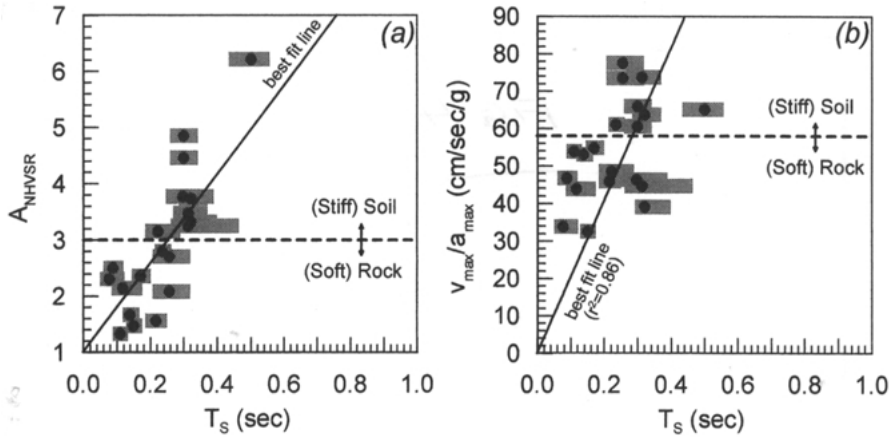

Figure 4. Correlation of NHVSR fundamental site periods with (a) the peak normalized elastic response spectra ratio A_{NHVSR}, and (b) the $v_{\max}/a_{\max}$ ratio. Dots depict the fundamental site period, while horizontal gray bars denote the significant period range where spectral ratio values are higher than 2/3 A_{NHVSR}.

cones and medium to well cemented conglomerates (THVC site) or neogene marls (ALIV site).

(b) *Soil – Stiff Soil formations*. It includes the remaining sites with A_{NHVSR} over 3, fundamental site periods T_{NHVSR} between 0.22 and 0.50 s, and $v_{\max}/a_{\max}$ ratio roughly over 58 cm s^{-1} g^{-1}. In geological terms, the formations of this category include moderately thick weathering products of the geological bedrock (ATHA and KERA site), alluvium deposits of medium to high density (ATH-02, ATH-03 and SPLB sites) or recent manmade deposits (MNSA site).

4. Site Response Analyses

The site response analyses were primarily performed in order to transfer seismic motions recorded on the free surface of soil sites to the surface of the outcropping bedrock, i.e., a hypothetical bedrock site at the location of the recording. At the sites where the seismic motion was recorded at depth (e.g., within subway stations), the analyses were used to estimate the seismic motion at the free surface of the overlying soil, and at the surface of the outcropping bedrock. In this way, actual recordings of the free ground motion were supplemented with site compatible analytical predictions and the total number of data points used to define the attenuation of seismic ground motion with distance from the fault rupture was substantially increased.

The theoretical model used to analyze the seismic soil response is shown in Figure 5: a number of horizontal soil layers, with non-linear visco-elastic response, resting upon a uniform, linear visco-elastic bedrock. Taking into account the geological structure of the wider area, the seismic bedrock was conventionally placed

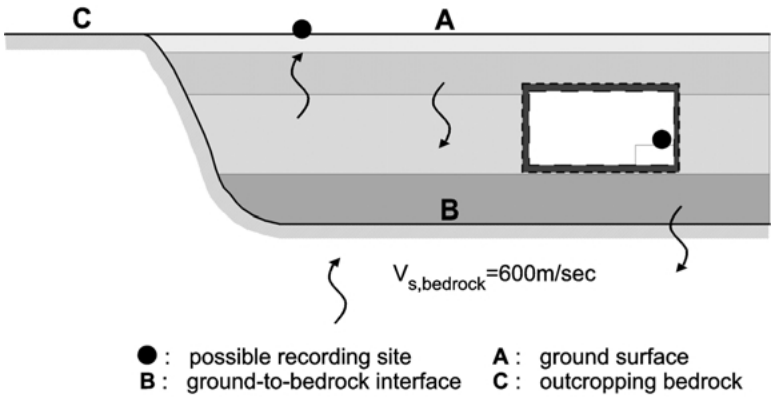

Figure 5. Soil and seismic bedrock model used for the seismic ground response analyses.

within neogene or older geological formations, with shear wave velocity greater than V_b = 600 m/s and mass density ρ = 2.2 Mg/m^3. The seismic excitation was introduced in the form of an acceleration time history, applied either at the free surface or within the soil profile at the depth of recording. Consequently, the site response was simulated with the equivalent-linear method (Schnabel *et al.*, 1972), assuming that earthquake-induced shear waves propagate vertically, from the seismic bedrock to the ground surface and vice-versa.

The seismic response analyses were performed for all recording sites listed in Table I, except from RFN, LAVR and ALIV, located at the towns of Rafina, Lavrion and Aliveri, respectively, where it has not become possible to collect any geotechnical data. In addition, no analyses were performed for recording site DMK, within Athens, laying directly upon bedrock formations, so that seismic ground motions could not have been affected by soil.

Definition of the soil properties required for the seismic response analyses faced two objective difficulties. The first is that geotechnical investigations were generally performed in the wider rather than the close vicinity of the recording sites, some times at 100–200 m distance. As a result, a possible range instead of specific values of soil properties was specified. The second difficulty is that the investigations did not include the special tests required to measure directly the dynamic soil properties. Hence, the shear wave velocity of the soil layers V_S was estimated indirectly from Standard Penetration Test measurements N_{SPT}, as (Imai and Tonuchi, 1982):

$$V_S(\mathrm{m/s}) = 97.0 N_{\mathrm{SPT}}^{0.314}. \tag{3}$$

The non-linear hysteretic response of soil to earthquake-induced dynamic shear deformations has been specified in connection to the plasticity index I_P, according to the empirical relations of Vucetic and Dobry (1991). A typical soil profile constructed with this procedure is shown in Figure 6. It is based on the geotechnical

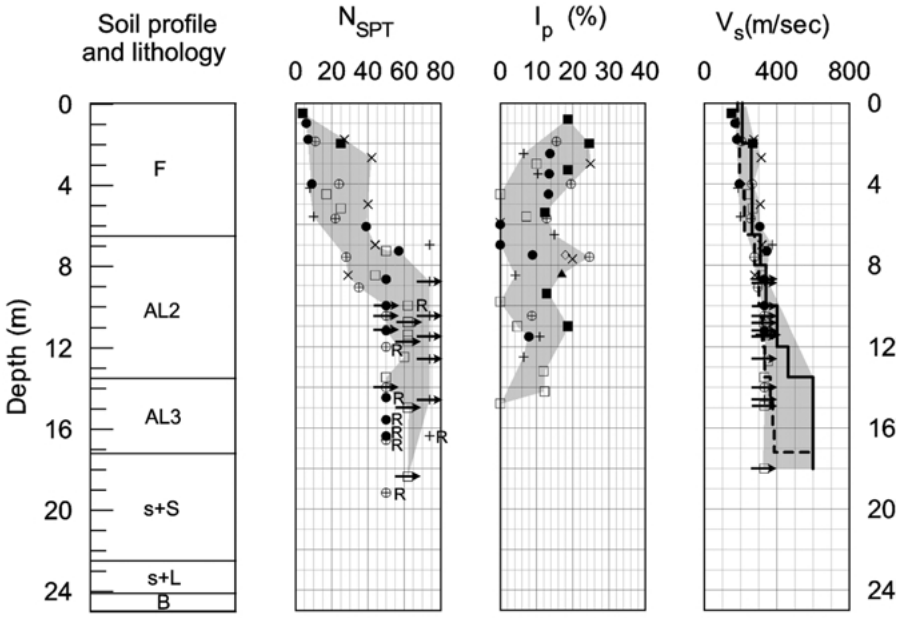

Figure 6. Geotechnical profiles for the SPLA and SPLB sites at Sepolia subway station. The continuous line shows the average V_S profile while the dotted line shows the scaled V_S profile used for the analysis of seismic ground response. Symbols and lithology notation are explained in the Appendix.

data collected for the wider area of Sepolia subway station, the location of two recording sites: SPLB on the free ground surface and SPLA at depth, within the station. The profiles for all recording sites are included in the Appendix.

Two analyses were initially performed for every recording site, one for each component of the seismic excitation, using the average soil properties denoted with bold line in the typical profile of Figure 6. For the sites with ground surface recordings, where fundamental site periods (T_{1-D}) obtained with this input data diverged more than about 10% from the periods obtained applying the NHVSR method (T_{NHVSR}), the analyses were repeated in order to improve agreement. The shear wave velocities used in the new analyses, denoted with dotted line in the typical profile of Figure 6, were obtained with a more or less uniform scaling of the initial values without violating the range of data obtained from the geotechnical investigations. From the total number of eight (8) sites with ground surface recordings, six (6) had to be re-examined with appropriately scaled shear wave velocities.

5. Analytical Predictions of Ground Response

To obtain a gross feeling of the accuracy associated with the analytical predictions, Figure 7 compares predicted and recorded seismic ground motions at the area of

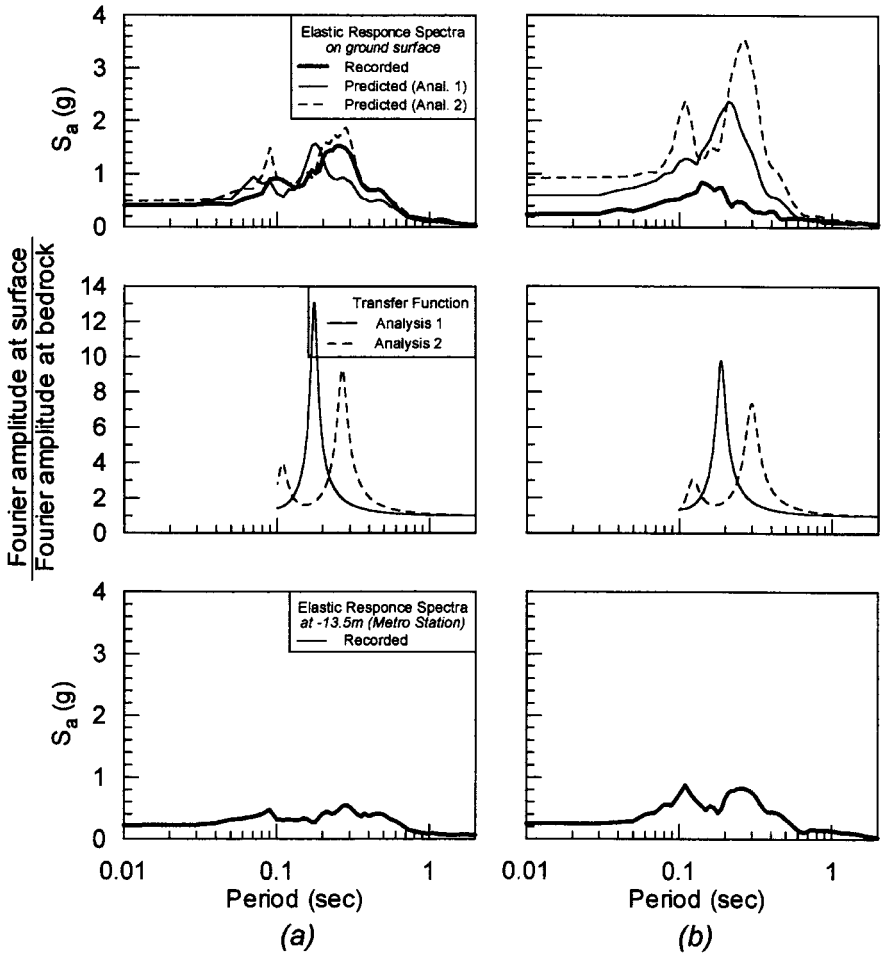

Figure 7. Comparison between typical analytical predictions and ground surface recordings at Sepolia subway station. Recorded motions within the station (SPLA) were used as input excitations while recorded motions at the ground surface (SPLB) were used to compare with the analytical predictions. The comparison is shown for (a) the TRANS component and (b) the LONG component of motion (parallel to the station).

Sepolia subway station. At this area, the seismic motion has been recorded at two sites 170 m apart, SPLB and SPLA, the first located at the ground surface and the second at approximately 14 m depth, within the subway station. The analyses were performed for the average (analysis 1) as well as the scaled (analysis 2) soil properties shown in Figure 6. The seismic motions recorded within the station (SPLA) were used as input excitation while the seismic motions recorded on the ground surface were compared with the analytical predictions. The comparison is shown in terms of the elastic response spectra for 5% damping.

It is observed that the numerical analyses for average soil properties predict a predominant site period of 0.18–0.19 s as compared to the 0.30 s obtained by the NHVSR method for the ground surface recording at SPLB. This difference is practically eliminated after an average 15% decrease of the shear wave velocity values. Predicted and recorded elastic response spectra compare fairly well for the TRANS component of the seismic motion, oriented perpendicular to the longitudinal axis of the subway station. For the LONG component, oriented parallel to the longitudinal axis of the station, the two sets of data show larger differences that are not improved after modification of the shear wave velocity values. This is a possible indication of interaction phenomena between the relatively stiff reinforced concrete skeleton of the station and the surrounding soil.

The basic results from all ground response analyses are summarized in Table III, for both the average and the scaled shear wave velocity profiles. The following information is provided for each recording site and each component of excitation (LONG, TRANS):

- the fundamental site period,
- peak accelerations at the free surface of the ground and the outcropping bedrock, as well as,
- the average spectral accelerations for period range 0.10–0.25 s and 0.25–0.50 s, where most of the damaged buildings belong.

Peak ground and average spectral accelerations for recorded motions are shown in bold characters, in order to be easily distinguished from the numerical predictions shown in plain characters.

Figure 8 compares analytically predicted fundamental site periods to site periods obtained directly from the NHVSR method. The data corresponding to the TRANS components of MNSA and ATH-02 records have been excluded from the comparisons, as possibly affected by dynamic soil-structure interaction phenomena. Observe that the fundamental site periods (T_{NHVSR}) correlate well to analytical predictions based on average shear wave velocity but they are systematically overpredicted by an average of 35% (Figure 8a). This difference is essentially eliminated when the shear wave velocity profile is scaled to lower values (Figure 8b). The average reduction applied to each recording site to close the gap varies merely between 5% and 20% and has a relatively minor effect on predicted ground and spectral accelerations.

At present, there is no conclusive evidence on the reasons for the observed difference in the fundamental periods derived with the two methods. However, taking into account that the methods are based on widely different concepts, it would be reasonable to oversee this bias as relatively small and emphasize that both sets of data reflect local ground conditions fairly well.

Table III. Summary of results from the seismic ground response analyses

Recording	Component	T_S (s)	T_S (fit)	a_{max} surface (g)	a_{max} bedrock out (g)	a_{max} bedrock out (fit)	Sa (g) surface ($0.10 < T < 0.25$)	Sa (g) surface ($0.25 < T < 0.50$)	Sa (g) bedrock ($0.25 < T < 0.50$)	Sa (g) bedrock ($0.10 < T < 0.25$)	Sa (a) bedrock out (fit) ($0.25 < T < 0.50$)	Sa (g) bedrock out (fit) ($0.10 < T < 0.25$)
ATHA	Long	0.25	0.31	**0.083**	0.046	0.044	**0.202**	**0.166**	0.120	0.123	0.120	0.100
	Trans			**0.101**	0.067	0.066	**0.260**	**0.229**	0.161	0.163	0.163	0.131
MNSA	Long	0.29	–	**0.233**	0.170	–	**0.448**	**0.420**	0.358	0.343	–	–
	Trans			**0.511**	0.407	–	**1.280**	**0.296**	0.223	0.946	–	–
SPLB	Long	0.20	0.28	**0.239**	0.143	0.150	**0.897**	**0.710**	0.233	0.361	0.350	0.189
	Trans			**0.407**	0.310	0.234	**0.803**	**0.726**	0.732	0.688	0.597	0.562
ATH-02	Long	0.22	0.28	**0.110**	0.081	0.075	**0.306**	**0.233**	0.167	0.216	0.196	0.135
	Trans			**0.159**	0.113	–	**0.533**	**0.174**	0.118	0.363	–	–
ATH-03	Long	0.13	0.23	**0.265**	0.234	0.209	**0.638**	**0.376**	0.350	0.486	0.455	0.311
	Trans			**0.302**	0.236	0.182	**0.820**	**0.501**	0.409	0.692	0.566	0.333
ATH-04	Long	0.19	0.24	**0.121**	0.089	0.089	**0.248**	**0.275**	0.234	0.182	–	–
	Trans			**0.110**	0.069	0.069	**0.226**	**0.203**	0.160	0.153	–	–
KERA	Long	0.22	0.30	**0.223**	0.172	0.159	**0.429**	**0.465**	0.337	0.274	0.288	0.251
	Trans			**0.186**	0.118	0.154	**0.586**	**0.347**	0.237	0.329	0.368	0.177
SPLA	Long	0.20	0.30	0.595	0.383	0.450*	1.849	0.858	0.637	1.058	1.209	0.858
	Trans			0.398	0.284	0.356*	1.059	0.624	0.493	0.593	0.618	0.554
SGMA	Long	0.32	–	0.219	0.174	–	0.641	0.372	0.269	0.447	–	–
	Trans			0.209	0.123	–	0.497	0.224	0.158	0.330	–	–
SGMB	Long	0.32	–	0.357	0.223	–	0.831	0.862	0.539	0.540	–	–
	Trans			0.263	0.184	–	0.537	0.898	0.587	0.349	–	–
DFNA	Long	0.10	–	0.064	0.045	–	0.144	0.076	0.073	0.116	–	–
	Trans			0.111	0.087	–	0.212	0.126	0.121	0.174	–	–
PNT	Long	0.25	–	0.285	0.186	–	0.979	0.254	0.176	0.563	–	–
	Trans			0.309	0.194	–	1.070	0.298	0.206	0.603	–	–
FIX	Long	0.12	–	0.224	0.185	–	0.534	0.146	0.143	0.448	–	–
	Trans			0.280	0.233	–	0.738	0.247	0.242	0.636	–	–
THVC	Long	0.10	–	**0.058**	0.055	–	**0.163**	**0.150**	0.148	0.156	–	–
	Trans			**0.056**	0.054	–	**0.149**	**0.112**	0.110	0.145	–	–

*Analysis of recording SPLA with soil profile (2) gave _max at ground surface 0.927 and 0.499 g for Long and Trans components, respectively.

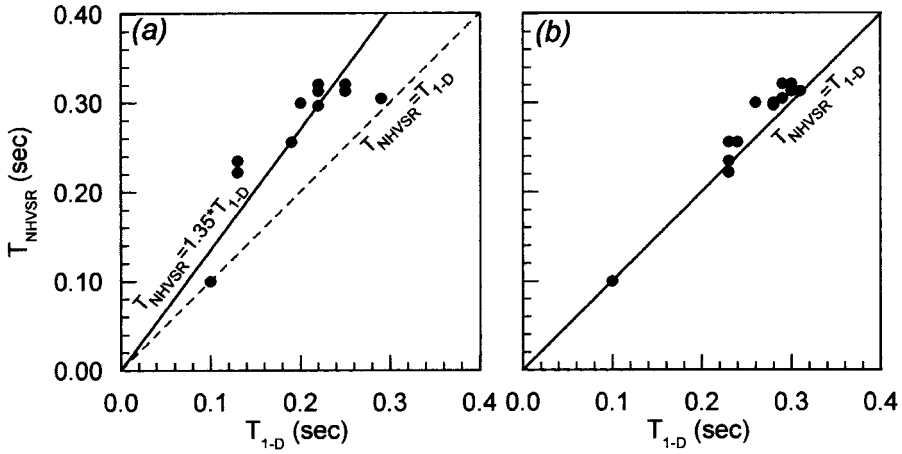

Figure 8. Comparison between fundamental site periods obtained from seismological data and site periods computed for (a) average V_S profiles and (b) scaled V_S profiles.

Attenuation of Seismic Ground Motion

Peak horizontal and vertical ground accelerations are correlated to the distance from the rupture in Figures 9 and 10, respectively. Similarly, Figures 11 and 12 show the effect of distance on the average normalized spectral accelerations for the two period ranges, 0.10–0.25 s and 0.25–0.50 s. All correlations are shown separately for Rock and Soil sites and include data obtained directly from the seismic recordings or indirectly from the site response analyses for the initial (average) soil velocity profiles. In all figures the available data are compared to the empirical relations from Abrahamson and Silva (1997) for the hanging wall of shallow crustal earthquakes of $M = 5.9$ magnitude. Since all recordings correspond to intermediate or large distances from the rupture, these relations are used to guide the extrapolation of available data to the epicentral area (shaded band).

The average values of the peak and the normalized spectral accelerations estimated in this way for Rock and Soil conditions are summarized in Table IV for different distances from the fault rupture. The effect of soil conditions is evaluated quantitatively with the aid of the Soil Amplification Ratio (SAR), defined as the ratio of peak ground accelerations at the soil surface and at the outcropping bedrock. Observe that soil effects become eminent for peak horizontal and average spectral accelerations only, whereas peak vertical accelerations are not significantly affected by local ground conditions. Estimated SAR values range between 1.34 and 1.96 for peak horizontal ground accelerations, increasing in general with the distance from rupture. The corresponding range for the normalized spectral accelerations is 0.96–0.99 for short periods and 1.13–1.37 for longer periods, with practically no systematic dependence on distance.

The previous data suggest that, while peak horizontal and vertical accelerations attenuate with distance from the fault, normalized spectral accelerations remain

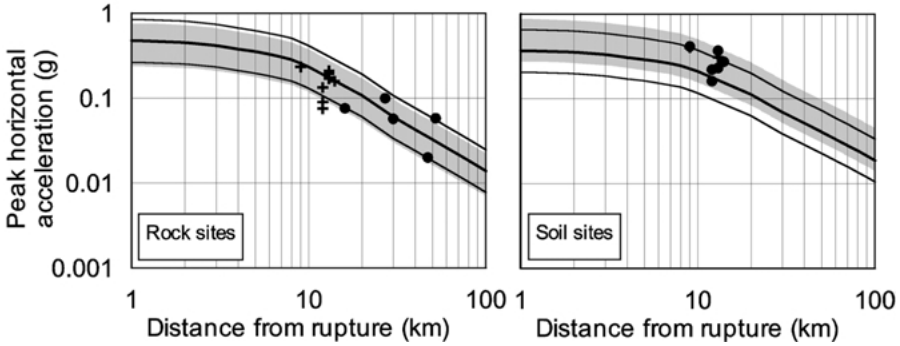

Figure 9. Attenuation of peak horizontal acceleration with distance from fault rupture for Rock and Soil sites. The continuous lines show the empirical relations (mean ± standard deviation) of Abrahamson and Silva (1997) for similar seismotectonic conditions. The gray band corresponds to the range of these relations but it has been translated vertically to fit the data points.

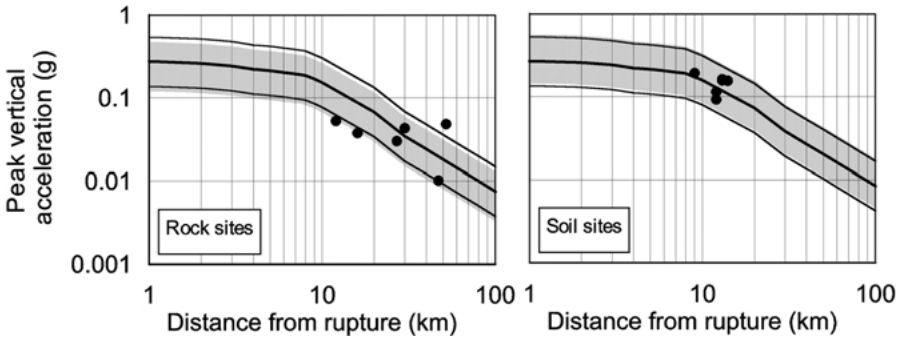

Figure 10. Attenuation of peak vertical acceleration with distance from the fault rupture. The presentation follows the format of Figure 9.

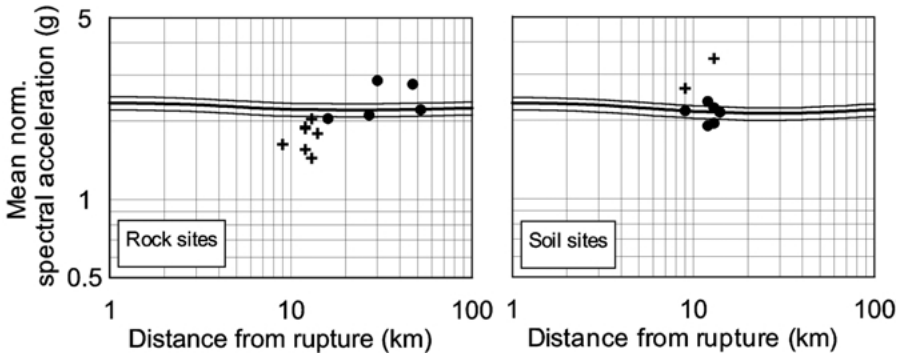

Figure 11. Attenuation of mean normalized spectral acceleration (T = 0.10–0.25 s) with distance from the fault rupture for Rock and Soil sites. The continuous lines show the empirical relations (mean + standard deviation) of Abrahamson and Silva (1997) for similar seismotectonic conditions.

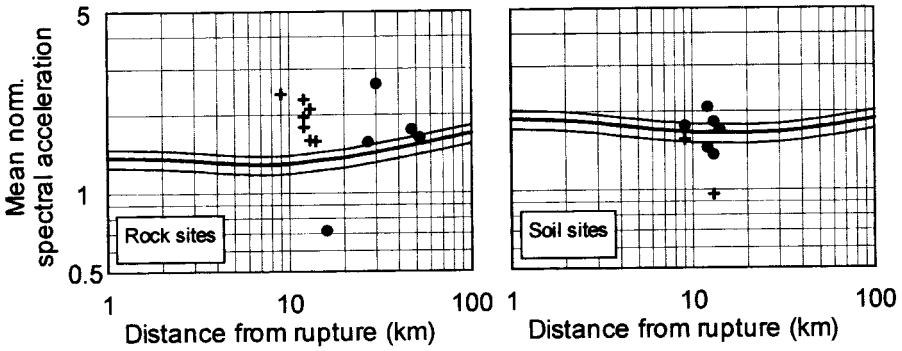

Figure 12. Attenuation of mean normalized spectral acceleration (T = 0.25–0.50 s) with distance from the fault rupture. The presentation follows the format of Figure 11.

Table IV. Estimated mean seismic motion parameters for different distances from the fault rupture.

Distance from rupture (km)		1	3	5	10	30	50
Peak vertical	ROCK	0.27	0.22	0.19	0.16	0.032	0.019
acceleration (g)	SOIL	0.30	0.25	0.22	0.18	0.042	0.022
	SAR	1.11	1.14	1.16	1.13	1.31	1.16
Peak horizontal	ROCK	0.42	0.35	0.32	0.20	0.048	0.028
acceleration (g)	SOIL	0.57	0.49	0.43	0.29	0.090	0.055
	SAR	1.357	1.400	1.344	1.425	1.875	1.964
Mean normalized spectral	ROCK	2.348	2.307	2.265	2.214	2.206	2.218
acceleration for	SOIL	2.329	2.281	2.229	2.158	2.119	2.140
$0.10 < T < 0.25$ s	SAR	0.992	0.989	0.984	0.975	0.961	0.965
Mean normalized spectral	ROCK	1.374	1.331	1.298	1.293	1.432	1.532
acceleration for	SOIL	1.887	1.803	1.728	1.658	1.662	1.730
$0.25 < T < 0.50$ s	SAR	1.373	1.354	1.331	1.282	1.161	1.130

practically constant. Based on this finding, Figure 13 shows the general shape of the normalized acceleration spectra for Rock and Soil sites, obtained as the average of the response spectrum from all available ground surface recordings, regardless of distance from the rupture. Notice that the seismic ground motions for Rock sites are rich in periods between 0.07 and 0.30 s with predominant period approximately equal to 0.10 s. For Soil sites, the range of important periods is between 0.10 and 0.40 s with predominant period of the order of 0.25 s. The aforementioned periods are of the same order with the fundamental period of 1–5 stories reinforced concrete buildings, commonly build in the wider Athens area and this may be one reason for the extensive damages caused by the earthquake.

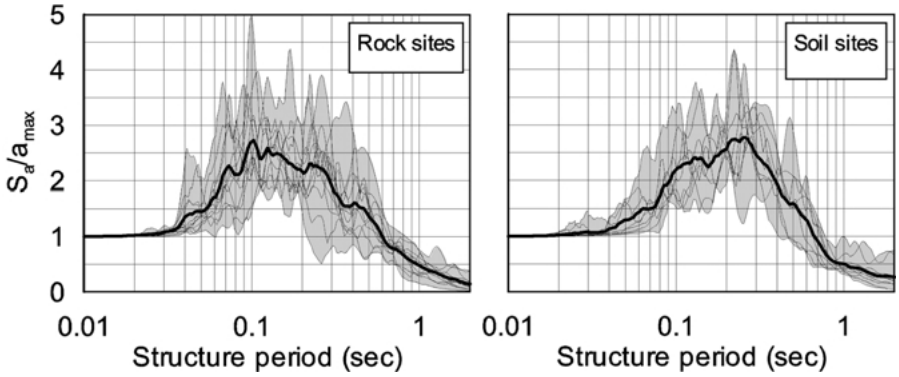

Figure 13. Normalized elastic response spectra (5% damping) for Rock and Soil sites. The shaded area shows the range of ground surface recordings and the thick line shows the average spectrum.

At the epicentral area, 1-3 km away from the fault rupture, peak vertical accelerations are grossly estimated as 0.22–0.27 g for Rock sites and 0.25–0.30 g for Soil sites. Peak horizontal accelerations are estimated as 0.35–0.42 g and 0.49–0.57 g for Rock and Soil sites respectively. Taking further into account the average normalized response spectra of Figure 13, the maximum mean spectral accelerations ($0.10 < T < 0.25$) at the same area are estimated as 0.810-0.98 g for Rock sites and 1.09–1.32 g for Soil sites. The above accelerations are statistically mean values and may have been locally exceeded by as much as 70%. Still, they are more than double compared to the values defined by the Greek National Seismic Code (EAK, 2000) for the wider Athens area.

6. Conclusion

The main findings of this study are briefly outlined below, with reference to the practical issues addressed in the introduction.

(a) *Principal direction of ground shaking.* It has been found that maximum recorded peak ground accelerations aim at an average direction 109°N. This is practically parallel to the rupture plane obtained from recently reported credible fault plane solutions.

(b) *Seismological methods for site characterization.* There are two main conclusions regarding this issue. The first is that fundamental site periods obtained from the normalized horizontal to vertical elastic response spectra ratio (NHVSR) correlate reasonably well to local geological and geotechnical conditions. Site periods obtained from NHVSR are consistently higher than the relevant analytical predictions by about 35%, but they follow a remarkably similar trend. This gap was efficiently eliminated by a 5–20% decrease in the empirical average estimates of shear wave velocities for the recording sites. The second conclusion is that the peak value of NHVSR (A_{NHVSR}) is more

sensitive to soil conditions than the fundamental site period (T_{NHVSR}), and may be readily used as a site index. On the contrary, the v_{max}/a_{max} ratio is less sensitive than both A_{NHVSR} and T_{NHVSR}, and should be used with caution.

(c) *Effect of local soil conditions*. The soil formations of Athens basin have amplified the horizontal (peak ground and spectral) accelerations from the main shock relative to outcropping rock-soft rock formations. Soil effects on vertical peak ground acceleration were, as expected, not significant. For 10–15 km distance from the fault rupture, where most recordings were obtained, horizontal peak ground accelerations were amplified by an average of 40%. This effect was certainly unexpected, since the soil formations at the recording sites are fairly stiff and could be classified as bedrock according to current seismic codes (e.g., EC8, 2000 and the Greek National Seismic Code EAK, 2000). Bouckovalas and Kouretzis (2001a, b) provide a more detailed account on this aspect.

(d) *Seismic motion parameters at epicentral areas*. Estimated peak horizontal ground accelerations at epicentral areas 1 to 3 kM away from the fault are 0.35–0.42 g for Rock sites and 0.49–0.57 g for Soil sites. The corresponding vertical accelerations are 0.22–0.27 g for Rock sites and 0.25–0.30 g for Soil sites. Maximum mean spectral accelerations (for 5% damping) are estimated as 0.80–0.98 g for Rock sites and 1.09–1.33 g for Soil sites. Due to data scatter, the above values may have been locally exceeded even by 70%.

The last two findings are indirectly related to the assumed location of the fault plane, which may be refined upon completion of the relevant seismological studies. In this event, slight modification should also be expected to the quantitative estimates of soil amplification and seismic motion parameters at the epicentral area.

Acknowledgements

The analyses presented in the article are part of research sponsored by the Organization for Seismic Planning and Protection of Greece, the Technical Chamber of Greece and the National Technical University of Athens. The strong motion records were provided by the Geodynamic Institute of the National Observatory of Athens (NOAGI), the Institute of Engineering Seismology and Engineering Seismology (ITSAK) and the Public Power Corporation of Greece. In addition, Attiko Metro S.A. provided the geotechnical data for all subway stations where accelerographs were installed. These contributions are deeply acknowledged.

Appendix A: Geotechnical Profiles at Recording Sites

The geotechnical profiles used in the seismic response analyses are presented in the figures of this Appendix. Apart from the purpose of documenting the findings of this article, these data allow an independent evaluation of the strong motion recordings.

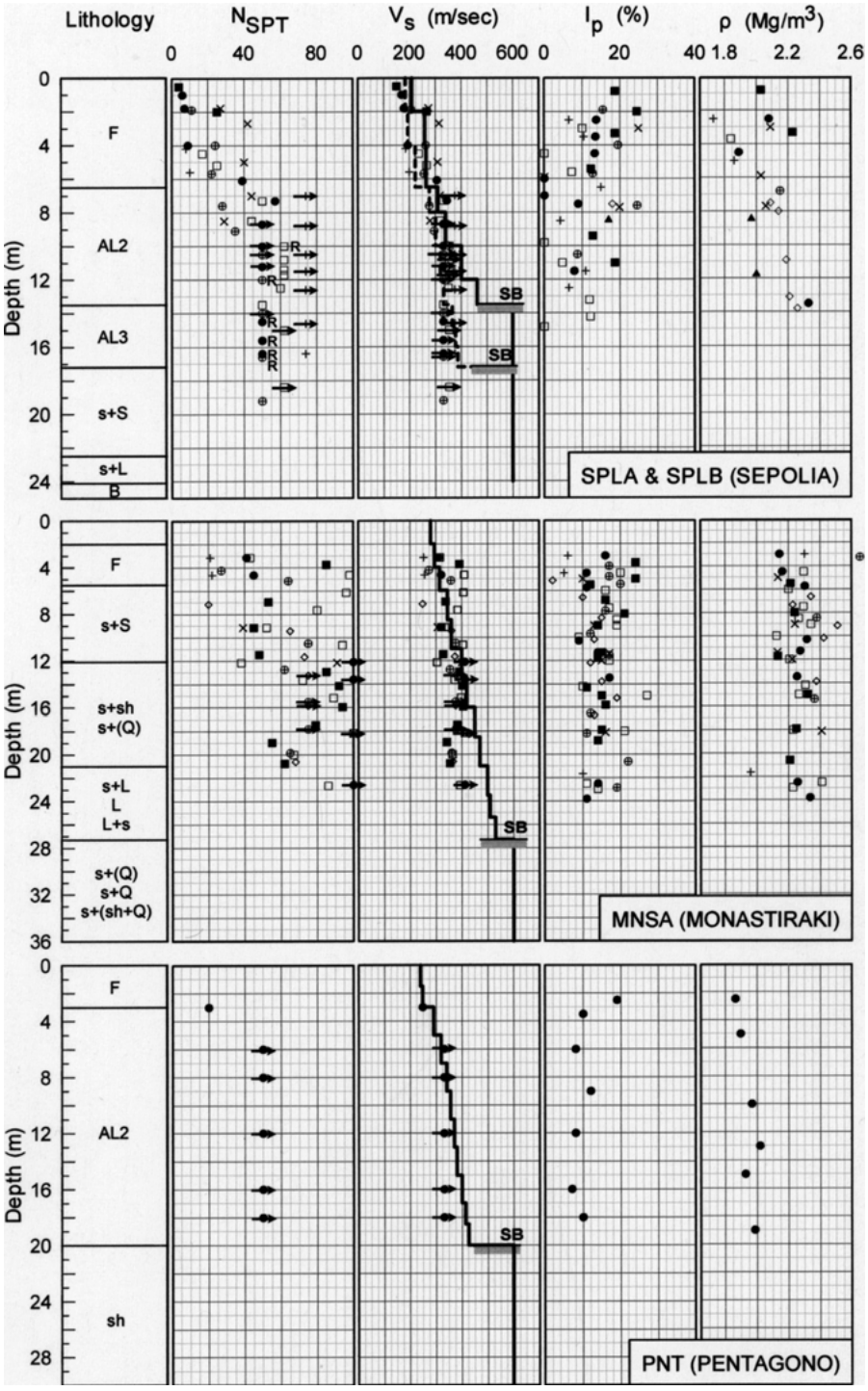
Lithology
N_{SPT}
V_s (m/sec)
I_p (%)
ρ (Mg/m^3)
Depth (m)
F
AL2
AL3
s+S
s+L
B
SB
SPLA & SPLB (SEPOLIA)
s+sh
s+(Q)
L
L+s
s+Q
s+(sh+Q)
MNSA (MONASTIRAKI)
sh
PNT (PENTAGONO)

Figure 1A.

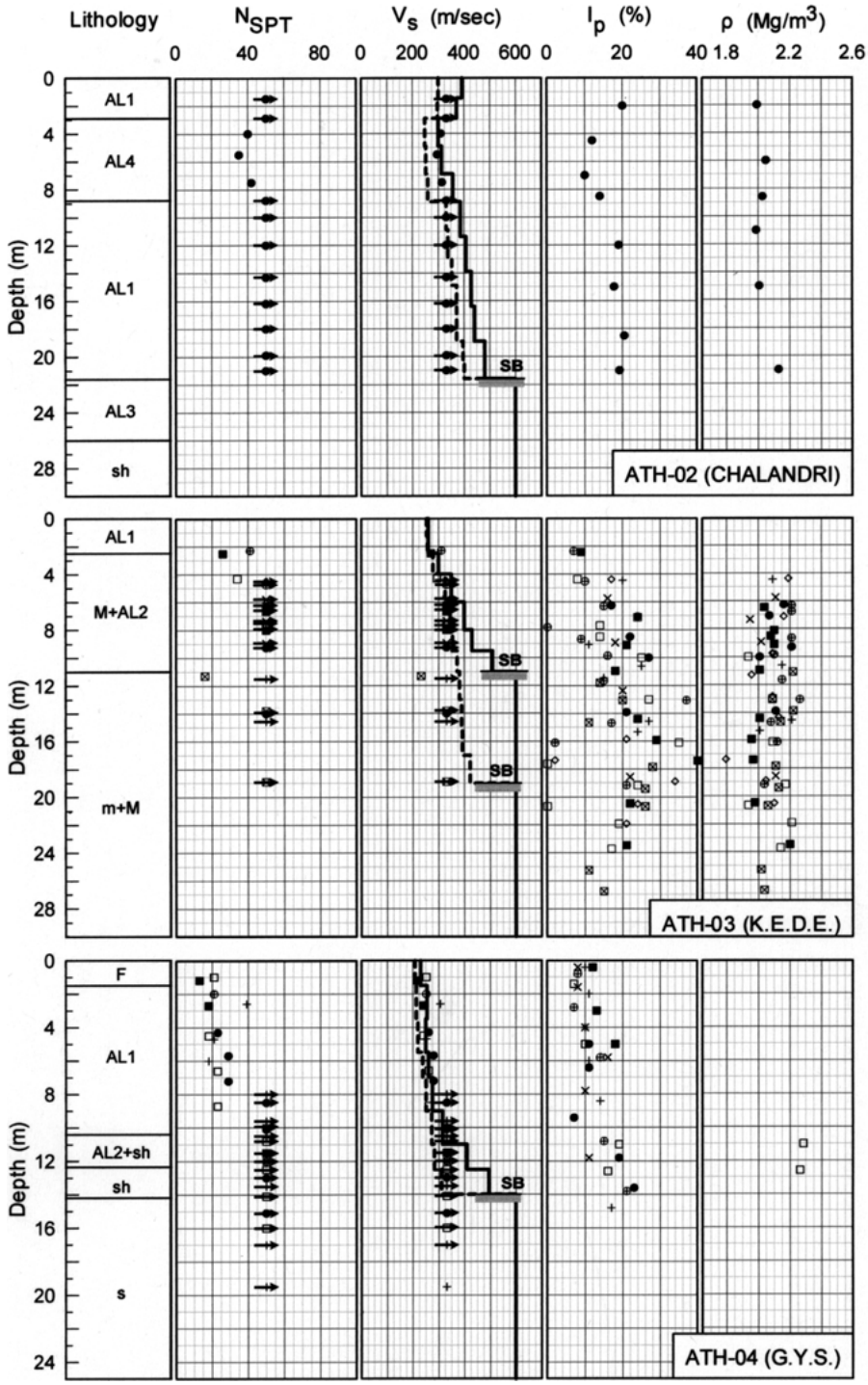
Lithology
N_SPT
V_s (m/sec)
I_p (%)
ρ (Mg/m3)
0 40 80
0 200 400 600
0 20 40
1.8 2.2 2.6
Depth (m)
AL1
AL4
AL1
AL3
sh
SB
ATH-02 (CHALANDRI)
AL1
M+AL2
m+M
SB
SB
ATH-03 (K.E.D.E.)
F
AL1
AL2+sh
sh
s
SB
ATH-04 (G.Y.S.)

Figure 2A.

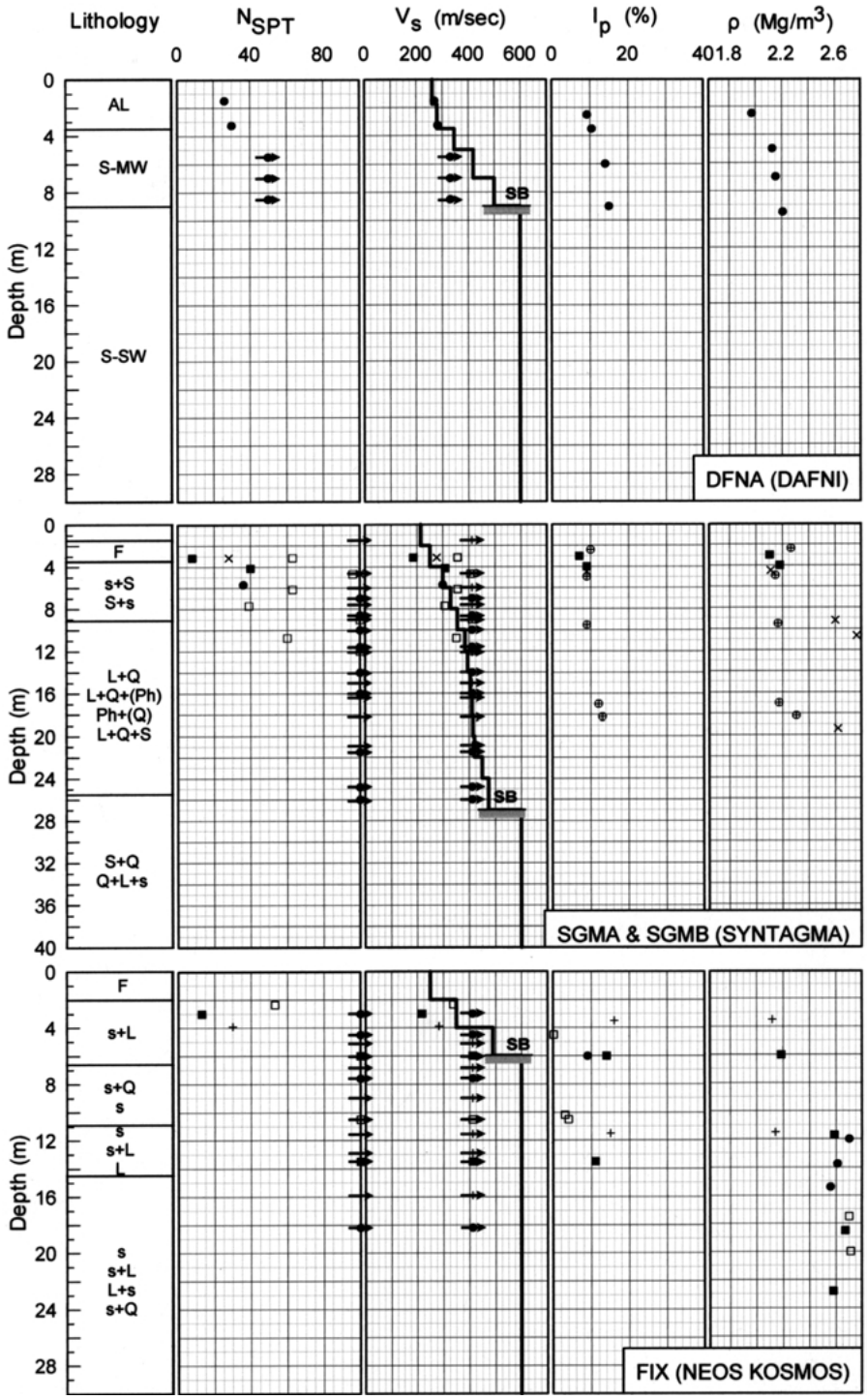
Lithology
N_{SPT}
V_s (m/sec)
I_p (%)
ρ (Mg/m^3)
0 40 80
0 200 400 600
0 20
1.8 2.2 2.6
Depth (m)
AL
S-MW
S-SW
SB
DFNA (DAFNI)
F
s+S
S+s
L+Q
L+Q+(Ph)
Ph+(Q)
L+Q+S
S+Q
Q+L+s
SB
SGMA & SGMB (SYNTAGMA)
F
s+L
s+Q
s
s
s+L
L
s
s+L
L+s
s+Q
SB
FIX (NEOS KOSMOS)

Figure 3A.

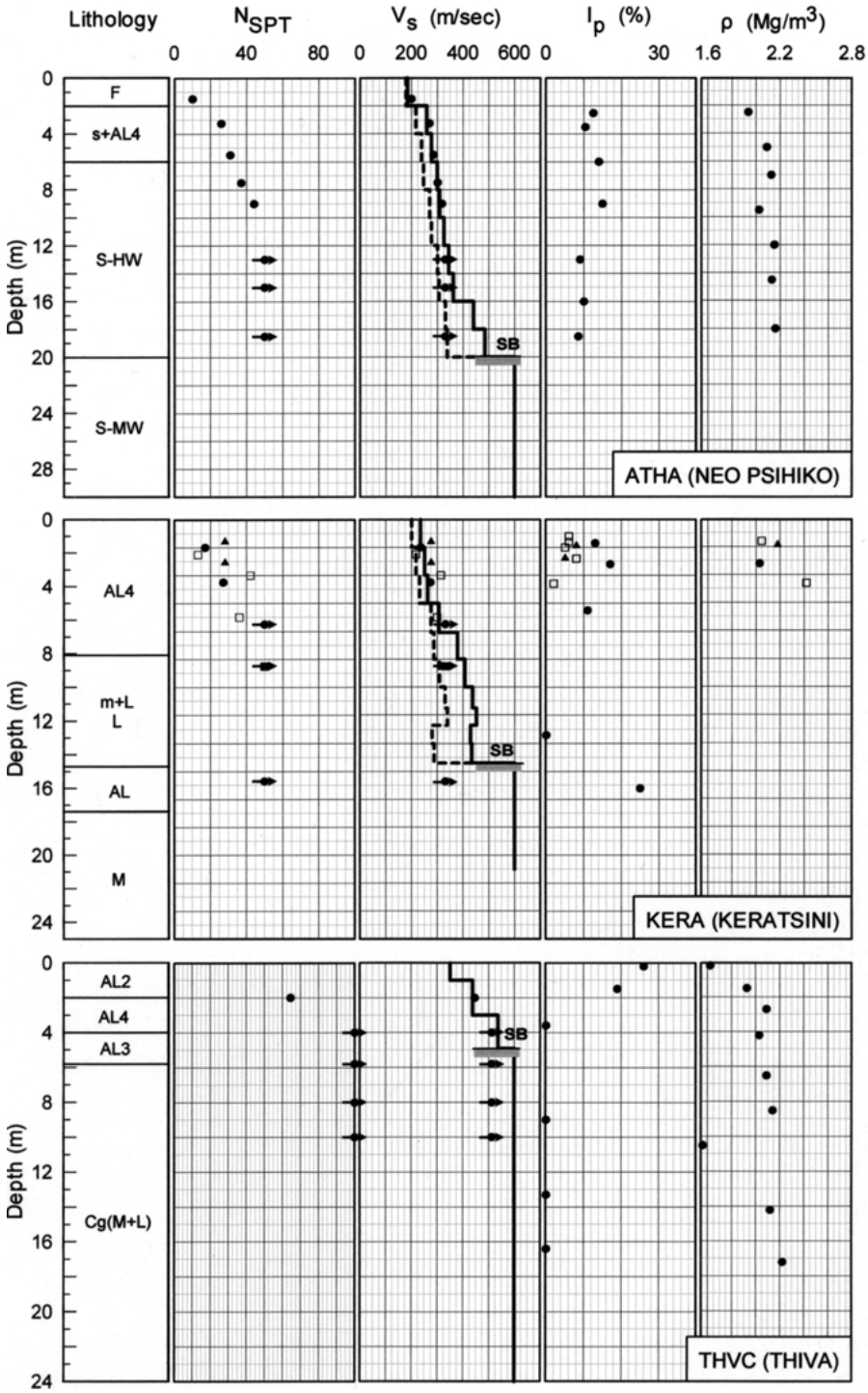
Lithology
N_SPT
V_s (m/sec)
I_p (%)
ρ (Mg/m3)
0 40 80
0 200 400 600
0 30
1.6 2.2 2.8
Depth (m)
F
s+AL4
S-HW
S-MW
SB
ATHA (NEO PSIHIKO)
AL4
m+L
L
AL
M
KERA (KERATSINI)
AL2
AL4
AL3
Cg(M+L)
THVC (THIVA)

Figure 4A.

Table A.1. Definition of lithology (obtained from the geological investigations for Attico Metro S.A.

UPPER DEPOSITS			
F:	Fill material		
AL (Alluvial deposits)			
AL1:	Silty clay to clayey silt (subrounded gravels)		
AL2:	Slightly to moderate cemented silty clay (gravel to pebble size subrounded particles)		
AL3:	Moderate to strongly cemented conglomerate		
AL4:	Poorly cemented conglomerate (sand to cobble particle size in a reddish clay matrix)		
Col/SD:	Colluvial deposits – Slope deposits		
AL/Col:	Non differentiated alluvial colluvial deposits		
SUBSTRATUM			
Pliocene – Pleistocene deposits:			
Cg(M + L):	Conglomerate (limestone pebble to cobble size particles in a reddish silty clay matrix)		
"Athenian schist" – Sedimentary origin			
NDS:	Non differentiated schist	sh:	Shales
M:	Marl	s:	Siltstone
S:	Sandstone	s + L:	Calcareous siltstone
S + L:	Calcareous sandstone	G:	Grauwacke
B:	Breccia	BL or (B + L):	Limestone breccia
m:	Marlstone	L:	Limestone
Q:	Quartz	Ph:	Phyllite
"Athenian schist" – Eruptive origin			
P:	Peridotite	D:	Diabase
Se:	Serpentine	Ps:	"Serpentinized" peridotite
BP:	Peridotite breccia	F:	Faulted zone

Each profile includes the geological description of the different layers, the Standard Penetration Test results (N_{SPT}), the shear wave velocity (V_s), the plasticity index (I_P) and the mass density (ρ). The symbols used for the description of the various lithological units are explained in Table A.1. In the presentation of the test data different symbols are used in order to differentiate measurements obtained at different boreholes. In the presentation of SPT results right arrows were used when a maximum number of blow counts was reached with penetration less than the 30 cm specified for termination of the test. In the same data, R denotes that no penetration was achieved during the test. The data regarding shear wave velocities

have been deduced indirectly from N_{SPT}, according to the empirical relations proposed by Imai and Tonuchi (1982) as described in the main text. In this case, the arrows denote lower limit values of V_s obtained from SPT results with partial or no penetration. The continuous black line denotes the average velocity profile while the dashed black line the profile used to fit the fundamental site periods suggested by the seismological data.

References

Abrahamson, N. A. and Silva,W.: 1997, *Empirical Response Spectral Attenuation Relations for Shallow Crustal Earthquakes*, Seismological Research Letters, Volume 68, Number 1, January/February.

Bonilla, F. L., Steidl, J. H., Lindley, G. T., Tumarkin, A. G., and Archuleta, R. J.: 1997, Site amplification in the San Fernando Valley, CA: Variability of site effect estimation using the S-wave, Coda and H/V methods, *BSSA* **87**, 710–730.

Bouckovalas, G. D. and Kouretzis, G. P.: 2001a, *Review of Soil and Topography Effects in the September 7, 1999 Athens (Greece) Earthquake*, Invited Lecture. Fourth International Conference on Recent Advances in Geotechnical Earthquake Engineering and Soil Dynamics. San Diego, California, 26–31 March, Vol. 2, 249–256 (in Greek).

Bouckovalas, G. D. and Kouretzis, G. P.: 2001b, *Stiff Soil Amplification Phenomena during Athens (07/09/1999) Earthquake*, 4th Hellenic Conference on Geotechnical and Geoenvironmental Engineering. Athens, 31 May–1 June.

Dimitriou, P., Kalogeras, I., and Theodoulidis, N.: 1999, Evidence of nonlinear site response in horizontal-to-vertical spectral ratio from near-field earthquakes, *Soil Dynamics and Earthquake Engineering* **18**, 423–435.

Dobry, R., Idriss, I. M. and Power, M. S.: 2000, New site coefficients and site classification system used in recent building seismic code provisions, *Earthquake Spectra* **16**, 41–67.

Donovan: 1989, *A Review of Spectral Attenuation Relationships*, Annual meeting of the Seismological Society of America, Victoria B.C., 21 April.

EAK: 2000, *Greek National Seismic Code* (in Greek).

EC8: 2000, *Design Provisions for Earthquake Resistance of Structures, Part 1-1: General Rules-Seismic Actions and General Requirements for Structures* (Draft), prEN 1998-5, European Committee for Standardization, Brussels.

Imai, T. and Tonuchi, K.: 1982, *Correlation of NSPT Value with S-Wave Velocity and Shear Modulus*, Proceedings of the 2nd European Symposium on Penetration Testing, Amsterdam, 24–27 May.

Joyner, W. B., Furnal, T. E., and Glassmoyer, G.: 1994, Empirical spectral response issues from an eastern U.S. perspective, In: G. R. Martin (ed.), *Proceedings of the 1992 NCEER/SEAOC/BSSC Workshop on Site Response during Earthquakes and Seismic Code Provisions*, University of Southern California, Los Angeles, 18–20 November, 1992, National Center for Earthquake Engineering Research Special Publication NCEER-94-SP01, Buffalo, NY.

Kalogeras, I. and Stavrakakis, G.: 1999, *Processing of the Strong Motion Data from the September 7th, 1999 Athens Earthquake*, National Observatory of Athens, Geodynamic Institute, Publication No. 10 (CD-ROM).

Mucciarelli, M., Bettinali, F., Zaninetti, M., Vanini, M., Mendez, A., and Galli, P.: 1996, *Refining Nakamura's Technique: Processing Techniques and Innovative Instrumentation*, Proceedings of ESC Assembly, Reykjavik, September, pp. 411–416.

Nakamura, Y.: 1989, *A Method for Dynamic Characteristics Estimation of Subsurface Using Microtremors on the Ground Surface*, RTRI, Quarterly Report, Vol. 30, No. 1, Japan

Papadopoulos, G. A., Drakatos, G., Papanastasiou, D. *et al.*: 2000, *Preliminary Results about the Catastrophic Earthquake of 7 September 1999 in Athens, Greece*, Seismological Research Letters, Volume 71, Number 3, May/June.

Schnabel, P., Lysmer, J., and Seed, H. B.: 1972, *SHAKE: A Computer Program for Conducting Equivalent Linear Seismic Response Analysis of Horizontally Layered Soil Deposits*, Earthquake Engineering, Research Center, University of California in Berkeley, Report No. UCB/EERC 72/12.

Theodoulidis, N., Archuleta, R. J., Bard, P. Y., and Bouchon, M.: 1996, *Horizontal-to-Vertical Spectral Ratio and Geological Conditions: The case of Garner Valley Downhole Array in Southern California*, Bulletin of the Seismological Society of America, pp. 1692–1703.

Trifunac, M. D. and Todorovska, M. I.: 2000a, Can aftershock studies predict site amplification factors? Northridge, CA, earthquake of 17 January 1994, *Soil Dynamics and Earthquake Engineering* **19**, 233–251.

Trifunac, M. D. and Todorovska, M. I.: 2000b, Long period microtremors, microseisms and earthquake damage: Northridge, CA, earthquake of 17 January 1994, *Soil Dynamics and Earthquake Engineering* **19**, 253–267.

Vucetic, M. and Dobry, R.: 1991, Effect of soil plasticity on cyclic response, *Journal of Geotechnical Engineering, ASCE* **117**(1), 89–107.

Yamazaki, F. and Ansary, M. A.: 1997, On the stability of horizontal-to-vertical spectral ratio of earthquake ground motion, *Bull ERS* **30**, 27–44.